DOI 10.1007/s11223-017-9886-0
Strength of Materials, Vol. 49, No. 3, May, 2017

PLASMA CASE HARDENING OF WEAR-RESISTANT HIGH-CHROMIUM CAST IRON

V. G. Efremenko,[a,1] Yu. G. Chabak,[a] A. E. Karantzalis,[b] A. Lekatou,[b] I. A. Vakulenko,[c] V. A. Mazur,[a] and V. I. Fedun[a]

UDC 621.658.012.531

The effect of plasma parameters on the case hardening of wear-resistant high-chromium cast iron in different structural condition is studied. Correlation relations were established between the initial and finite microstructure of the surface layer formed after plasma hardening at different heating rates. Microhardness profiles over the cross-section of the modified layer are structurally substantiated. Recommendations for optimizing the complex bulk-surface cast iron treatment conditions are given.

Keywords: high-chromium cast iron, plasma hardening, austenite, martensite, hardness.

Introduction. The service life extension of tools and machine components is a challenge for modern materials science. One of the lines of its solution is the use of hardening technologies [1, 2] among which are surface modification methods with high-concentration heating sources (laser, electron-beam, plasma). Superhigh heating ($\sim 10^5$ ℃/s) and cooling rates can provide higher hardness, strength, and fracture toughness characteristics than on traditional thermal treatments. It is determined by the formation of highly dispersed martensite in surface layers, characterized by the higher density of imperfections and distorted crystal lattice [3]. Of the above methods plasma hardening is in most common use [3–5]. As is known, plasma jet heating is successfully used for hardening machine components, steel tools, hard alloys, gray iron castings. At the same time, the literature data on plasma hardening for modifying alloyed cast irons used as wear-, corrosion-, heat-resistant, nonmagnetic materials are lacking [6].

The plasma-case hardening is most efficient for special irons designed for operation under intensive wear conditions. As a rule, wear-resistant irons contain 10–25% Cr and other elements (Mn, Ni, V, Mo, Ti, Cu) improving the complex of mechanical properties [6, 7]. The structure of high-chromium irons consists of eutectic carbides and the metallic matrix, in as-cast condition they exhibit poor properties, therefore, they are subjected to bulk thermal treatment. The machinability of high-chromium irons is improved with annealing to obtain the ferrite-carbide structure [8], the wear resistance is increased with destabilizing hardening that forms the martensite or martensite-austenite matrix with dispersed secondary carbides [9, 10]. Thus, high-chromium irons are characterized by the microstructure of different types that can essentially influence the strengthening effect after plasma hardening. Since this issue is of great scientific and practical interest, the object of this study is to investigate the hardenability of wear-resistant high-chromium irons on plasma case hardening to suit the initial type of alloy microstructure.

1. Experimental Procedure. Iron, containing (%): 2.70 C, 14.55 Cr, 2.20 Mn, 0.55 Si, 0.93 Ni, 0.39 Mo, 0.38 V, 0.11 Ti, was investigated. Iron was melted out in a laboratory 20-kg induction furnace and poured into sand molds, producing bars of a 25×25 mm cross-section. The specimens were cut from the bars and ground to necessary dimensions ($10 \times 10 \times 25$ mm), then they were plasma-hardened both in the initial cast condition (C) and in the annealing condition from 950℃ followed by tempering at 200℃, 2 h (LT) or 600℃, 6 h (HT). Plasma hardening of the specimens was performed with an indirect plasmatron [3] of the following parameters: generator nozzle diameter

[a]Azov State Technical University, Mariupol, Ukraine ([1]vgefremenko@gmail.com). [b]University of Ioannina, Ioannina, Greece. [c]Lazaryan Dnepropetrovsk National Railway Transport University, Dnepr, Ukraine. Translated from Problemy Prochnosti, No. 3, pp. 126 – 135, May – June, 2017. Original article submitted February 10, 2016.

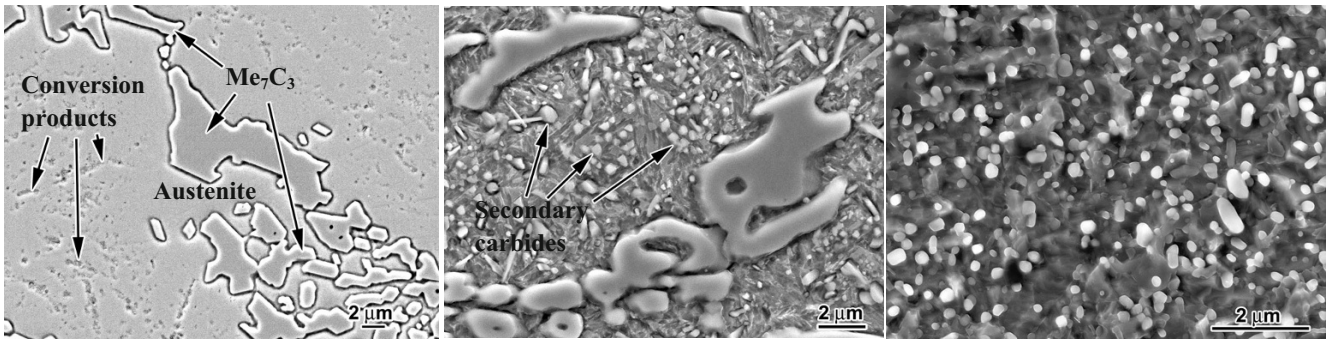

a b c

Fig. 1. Initial iron microstructure in C (a), LT (b), and HT (c) conditions.

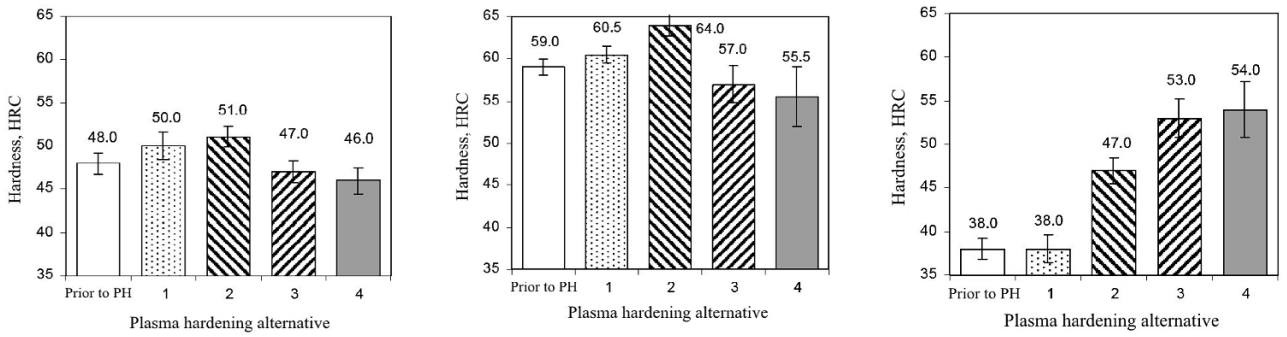

a b c

Fig. 2. Effect of plasma hardening on the hardness of iron in C (a), LT (b), and HT (c) conditions.

of 6 mm, arc length of 150 mm, argon as a plasma-generating gas (2 m^3/h flow rate), DC supply of 230–250 A at operating voltage of 55–60 V, plasma jet velocity (four alternatives): 0.6 (No. 1), 0.4 (No. 2), 0.33 (No. 3), and 0.25 m/min (No. 4). According to [11], the temperature of surface heating is ~ 800–900°C (No. 1), ~ 1000–1200°C (No. 2), ~ 1300–1400°C (No. 3), and ~ 1500–1550°C (No. 4). The microstructure of specimens was analyzed with an Axiovert 40 MAT optical microscope and JEOL JSM-6510LV scanning electron microscope. Hardness was measured with a Rockwell hardness meter, the microhardness distribution across the section of a modified layer was evaluated with a Shimadzu HMV-2 microhardness meter at a 50-g load.

2. Experimental Results.

2.1. Initial Cast Iron Microstructure and Hardness Variations. Prior to case hardening, the as-cast iron hardness was 48 HRC, after hardening and tempering at 200 and 600°C, it was 59 and 38 HRC, respectively. The microstructure of cast iron is the austenite+carbides Me_7C_3 eutectic and dendrites, consisting of austenite and its convesion products (Fig. 1a). After hardening and low tempering, the structure of dendrites is martensite-austenitic with dispersed inclusions of secondary carbides Me_7C_3 and $Me_{23}C_6$ (Fig. 1b), after hardening and high tempering, it is ferritic with grained carbides (Fig. 1c).

As a result of plasma hardening (Nos. 1 and 2) mean hardness in C condition increased to 50 and 51 HRC, respectively (Fig. 2a), after hardening (Nos. 3 and 4), it decreased to 47 and 46 HRC, respectively.

Plasma hardening of iron in LT condition (No. 1) leads to an increase in mean hardness by 1.5 HRC (to 60.5 HRC), even better effect was observed for alternative No. 2 (64 HRC, which is by 1.5 HRC higher than the hardness after untempered bulk hardening) (Fig. 2b). The hardness of iron on hardening (Nos. 3 and 4) goes down to 57 and 55.5 HRC, respectively.

The effect of plasma hardening on hardness is quite different for iron specimens in HT condition (Fig. 2c). Plasma hardening (No. 1) does not practically change the hardness level (38 HRC), with altematives Nos. 2, 3, and 4, it grows successively to 47, 53, and 54 HRC, respectively.

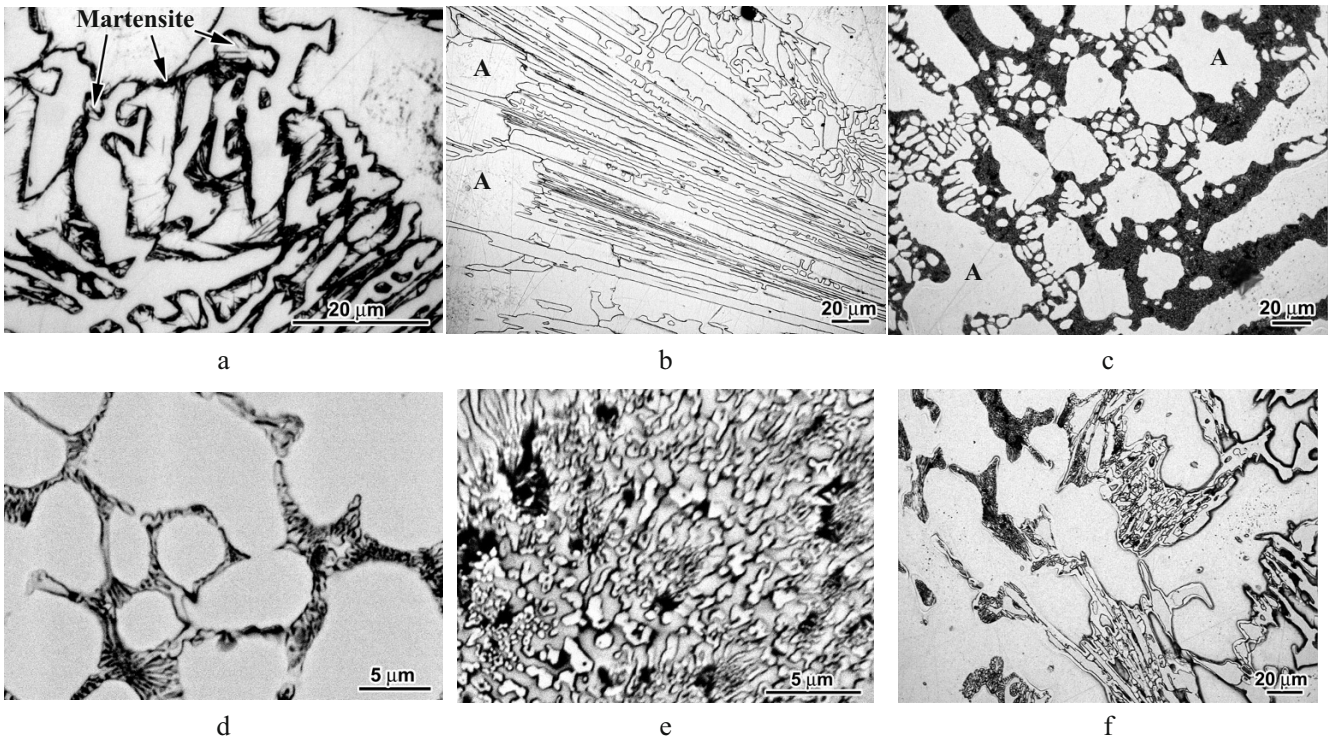

Fig. 3. Microstructure of iron in C condition after plasma hardening by Nos. 1 (a), 3 (b), 4 (c–f). (*A* – austenite.)

2.2. Structure and Microhardness of Plasma-Hardened Iron Layers.

2.2.1. Iron in C Condition. Fine-structural investigations show that plasma hardening (Nos. 1 and 2) does not almost change the microstructure as compared to that of the as-cast iron, except that fine-acicular martensite is formed along the contour of eutectic carbides in the subsurface layer 100 μm thick (Fig. 3a), the microstructure of deeper layers does not differ from that of as-cast iron. On hardening (No. 3), austenite decomposition products disappear in a layer 170–180 μm thick, in this layer the martensite "fringe" around eutectic carbides is also absent (Fig. 3b). For plasma hardening (No. 4), the microstructure of the surface iron layer changes greatly at the heating temperature to ~1500°C, with its local fusion to a depth of 170 μm. The fusion zone is very inhomogeneous as regards its dendritic structure: it consists of coarse (20–50 μm in diameter) dendrites of initial austenite and fine (2–10 μm) dendrites that came about from the liquid in fusion areas of former eutectic colonies (Fig. 3c). In this zone, a thin network of skeleton-like carbide eutectic appears along dendrite boundaries. It differs greatly from the initial eutectic in carbide sizes: if in the base structure, the cross-section of eutectic carbide fibers reaches 4–10 μm, in the new eutectic, it is only 0.1–0.5 μm (Fig. 3d).

A thin eutectic network moving away from the surface gives way to extensive areas of eutectic formed from fine (0.2–0.6 μm) rod-like carbides Me_7C_3 (Fig. 3e). Then the transition zone follows, with partially fused carbides of initial eutectic (Fig. 3f), after it the heat-affected zone is located (austenite decomposition products and martensite are absent), then the zone with the structure typical of the as-cast specimen is revealed.

Averaged curves of microhardness variations for dendritic iron areas over the cross-section of a modified layer for different plasma hardening alternatives are shown in Fig. 4. As follows from Fig. 4a, plasma hardening (No. 1) does not practically change the iron microhardness profile in C condition: at any distance from the surface, the microhardness makes up 520 $HV_{0.05}$ on the average, varying from 470 to 570 $HV_{0.05}$ in relation to the ratio of austenite and its decomposition products within a specific examined area.

Plasma hardening (No. 2) leads to an increase in the matrix microhardness to 640–660 $HV_{0.05}$ to a depth of 30 μm from the surface without apparent microstructure changes in this layer. After hardening (No. 3), at a depth of 150 μm the layer appears wherein the microhardness goes down to 450 $HV_{0.05}$ due to austenite formed without

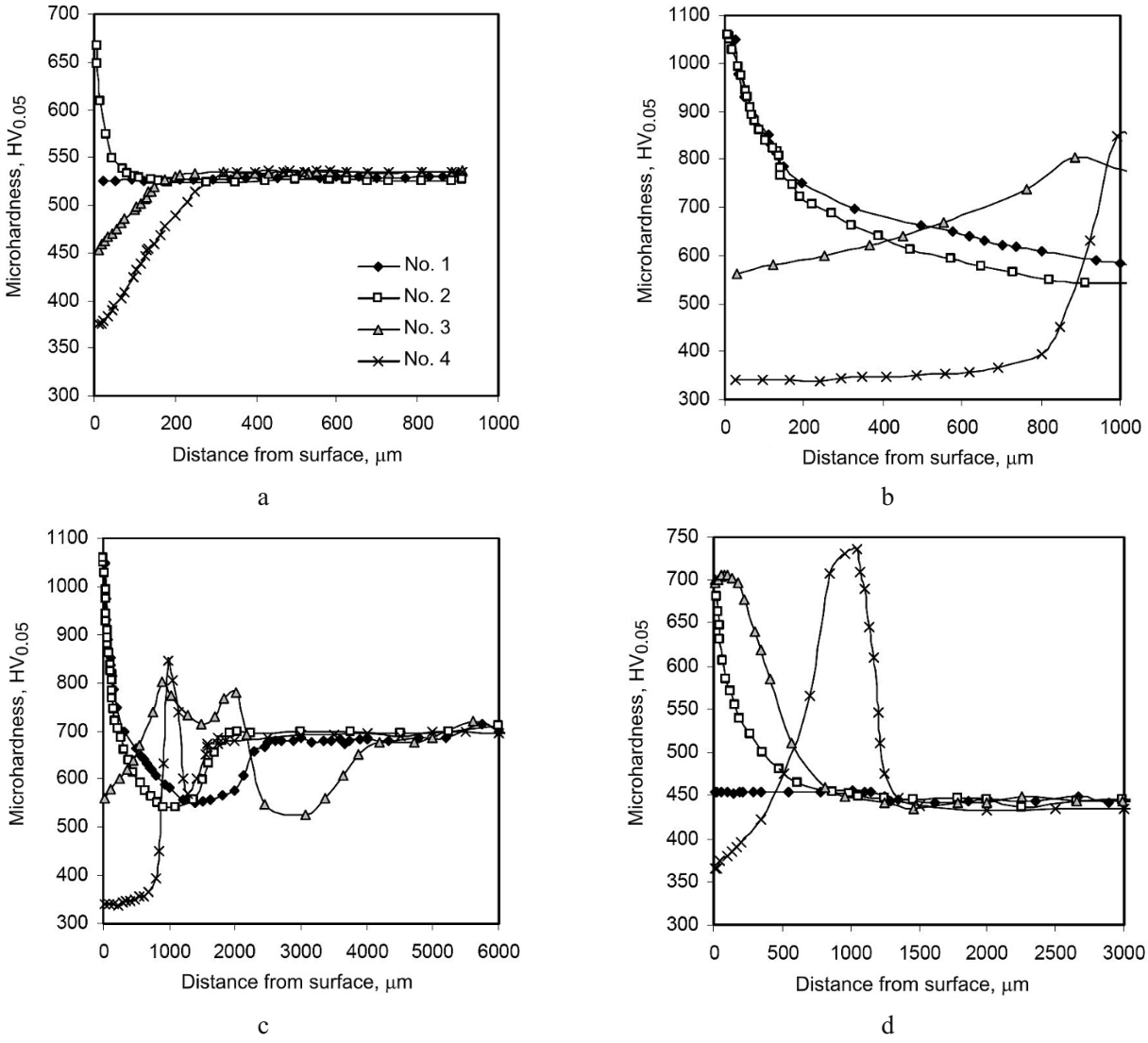

Fig. 4. Variation of the metallic matrix microhardness over the cross-section of specimens after plasma hardening: (a) iron in C; (b, c) LT condition; (d) HT condition [(*1*), (*2*), (*3*), (*4*) alternative numbers].

conversion products. The microhardness decreases still further (to 380 $HV_{0.05}$) in the fusion-affected layer after hardening (No. 4). Since in this case the matrix also consists of austenite, its lower (in comparison with No. 3) microhardness can be explained by that it is partially formed from the liquid, thus, did not undergo phase transformations, which could ensure its strain hardening [12] due to an increase in the density of imperfections of the crystal structure on phase working.

2.2.2. Cast Iron in LT Condition. Plasma hardening of iron in LT condition (Nos. 1 and 2) results in higher etching sensitivity of the subsurface layer on retention of a set of microstructure components (martensite, secondary carbides, residual austenite) typical of the initial condition (prior to plasma hardening). The intensification of etching is determined by a growth in the quantity of secondary carbides due to new, more dispersed inclusions (Fig. 5a). The subsurface layer width makes up 1000–1200 and 1700–1800 μm for Nos. 1 and 2 alternatives, respectively (Fig. 4b). Within those ranges, the microhardness is nonuniformly distributed: in a thin subsurface layer 30–40 μm wide, it reaches high values (1000–1080 $HV_{0.05}$), after that it starts decreasing gradually, giving way to a layer with low hardness (500–570 $HV_{0.05}$) at a certain depth (800–1100 μm – No. 1 and 1200–2200 μm – No. 2) (Fig. 4c). Then the microhardness increases, reaching a level typical of the unmodified structure of central layers (650–720 $HV_{0.05}$).

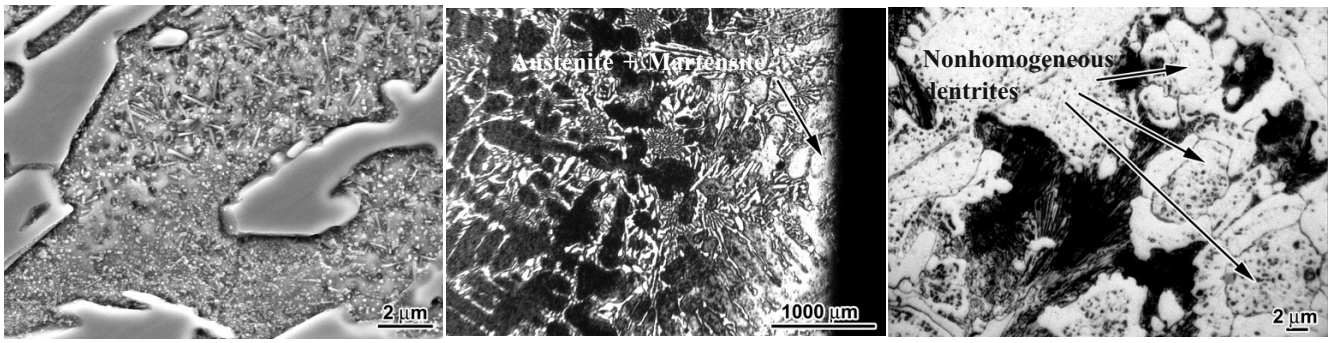

a b c

Fig. 5. Microstructure of iron in LT condition after plasma hardening by Nos. 2 (a), 3 (b), and 4 (c) alternatives.

After hardening (No. 3), on the surface (to 250 μm) a slightly etching layer arises wherein, judging by the microhardness (550–620 $HV_{0.05}$) and microstructure pattern, the austenite-martensitic matrix is formed with secondary carbide inclusions (Fig. 5b). When moring away from the surface, the structure is etched more intensively and its microhardness grows and reaches 800 $HV_{0.05}$ at a depth of 850–900 μm. The zone of higher microhardness extends to a depth of 2000 μm, approximately in its middle portion, the area is found where the microhardness is somewhat lower (710–730 $HV_{0.05}$). At a depth above 2000 μm, a "hard" layer gives way to the "soft" one wherein the microhardness does not exceed 600 $HV_{0.05}$. The initial level of microhardness is regained at a depth of ~ 4000 μm.

An increase in temperature on plasma hardening (No. 4) results in local fusion of the iron surface. In fused areas at a depth of 150–200 μm the zones appear wherein the microstructure is close to those, described above for iron in C condition. The exception is the heterogene structure of initial (coarse) austenitic dendrites consisting of the areas of lower (along the contour) and higher (in the center) etching sensitivity, separated with a thin carbide network (Fig. 5c). The mean microhardness of dendrites along the contour and in the center makes up 360 and 401 $HV_{0.05}$, respectively (Fig. 4b). Behind the fused layer, a layer is located with a sufficiently high hardness (800–850 $HV_{0.05}$), after it, a soft layer follows (~ 550 $HV_{0.05}$), giving way to the basic structure (660–690 $HV_{0.05}$). In those surface areas, where fusion does not occur, the microstructure and hardness over the cross-section of a modified layer are distributed about the same way as for alternative No. 3.

2.2.3. Cast Iron in HT Condition. Plasma hardening of iron in HT condition (No. 1) does not change the initial microstructure of the specimen: at different distances from the surface it is granular pearlite with microhardness of 430–480 $HV_{0.05}$ (Fig. 1c). Plasma hardening (No. 2) leads to an increase in microhardness to 600–670 $HV_{0.05}$ to a depth of 70 μm (Fig. 4d). Even a more pronounced effect was obtained after hardening (No. 3): microhardness of a modified layer grows to 680–720 $HV_{0.05}$ and its thickness reaches 300 μm. This layer possesses a dispersed dark-etching microstructure gradually transferring to granular pearlite at a distance from the surface. Plasma hardening (No. 4) results in the heterogene structure with alternating fused and unfused areas formed on the surface. The structure and microhardness of unfused areas are typical of alternative No. 3 and those of the fused ones are characteristic of iron in LT condition after alternative No. 4. In this case, microhardness profiles do not possess the tempering area revealed in the specimens of iron in LT condition after all plasma hardening alternatives.

3. Results and Discussion. The above results demonstrate that plasma hardening exerts different strengthening effects in accordance with the initial microstructural condition of high-chromium cast irons. Plasma hardening is the least effective procedure for as-cast high-chromium irons with the initial microstructure containing great quantities of primary austenite stable to the martensite transformation. To gain high hardness, the structure of a modified layer should be mainly martensite: the emergence of martensite is possible only after the isolation of a certain quantity of secondary carbides from austenite, which requires long holding at high temperatures [13]. At high heating and cooling rates, it does not occur, therefore, primary austenite does not undergo the martensite transformation. Moreover, on plasma hardening (Nos. 1 and 2), the inverse transformation of decomposition products to austenite even has no time to complete, which is indicative of the fact that the temperature range of the inverse phase transformation extends abruptly with a heating rate. Thus, plasma hardening by those alternatives does not practicaly

change the iron microstructure; gain in microhardness in a narrow subsurface layer to ~ 650 $HV_{0.05}$ after alternative No. 2 is explained by strain hardening of austenite due to thermal deformations on abrupt heating/cooling. On fusion, eutectic carbides are dissolved in the surface layer, the liquid is saturated with chromium and carbon, and on rapid crystallization, supersaturated stable austenite is formed, with a thin carbide eutectic crystallized along its boundaries. The total quantity of carbides is decreased, which in combination with the formation of the austenite matrix (without martensite and transformation products) leads to a reduction in hardness in relation to the initial condition. Thus, plasma hardening of as-cast high-chromium irons does not provide effective modification of the surface with its expected hardening.

A required strengthening effect of plasma hardening was obtained for iron in LT condition. The matrix of the as-cast iron contained optimum quantities of carbon and alloying elements reached by the isolation of secondary carbides on heating and holding. Thus, in this case the matrix was "prepared" for the martensite transformation. After plasma hardening (Nos. 1 and 2), iron in LT condition demonstrates an increase in the matrix microhardness to 1000–1080 $HV_{0.05}$, which is by 150–200 $HV_{0.05}$ higher than the hardness of martensite produced on bulk treatment. It is probably determined by the fineness of martensite crystals due to an abrupt reduction in critical austenite nucleus sizes on considerable surface overheating. Moreover, in the modified layer, the isolation of new, more dispersed secondary carbides is observed that provides an additional strengthening effect. It is believed that they were formed by the mechanism of dynamic strain ageing within the initial martensite areas in the locations of aggregation of crystal structure imperfections.

The distribution of microhardness over the cross-section of modified layers for iron in LT condition is controlled by the temperature gradient in the specimen on plasma heating. Temperatures above Ac_1 cause the phase recrystallization and (at sufficiently high temperature) dissolution of carbides, at lower temperatures, the initial martensite structure is decomposed. The latter results in a soft layer under the plasma-hardened one. The formation of a tempered layer in the plasma heat-affected zone is inevitable for the initial nonequilibrium structure, in this case, tempered martensite.

On plasma hardening (No. 3), the strengthering effect gives way to softening since temperature in the surface layer reaches the area of secondary carbide dissolution, which leads to the austenite stabilization, smaller hardened martensite quantities, therefore, to lower iron hardness. With a distance from the surface, the temperature becomes low to dissolve carbides, remaining sufficient for the recrystallization and martensite transformation, which generates the layer of higher hardness under the soft surface layer. A similar microhardness profile is also typical of the fused areas (No. 4), only in this case, the surface hardness is reduced even to a greater extent, behind the fused zone (austenite) the zone with partially dissolved carbides (austenite+martensite) is located, and just behind it, the hard zone with the martensite structure is observed. So, iron in LT condition at any plasma hardening alternative is characterized by a repeated change of modified layers with different microhardness. The alternating of fused and unfused areas results both in a decrease of mean surface hardness and in a wide scatter of its values, which caused an increase in the confidence interval from 1.2–1.5 to 2.5–3.0 HRC (Fig. 2b).

The structure of iron in HT condition features the concentration of practically all carbon in carbides (eutectic and secondary), therefore, a high hardness on the martensite transformation can be reached as a result of certain saturation of a solid solution with carbon due to the partial dissolution of secondary carbides. Plasma hardening (No. 1) does not ensure such dissolution, hence the iron hardness remains low. The above dissolution occurs at an increase in temperature on plasma hardening (No. 2): the modified layer of higher hardness arises on the surface. With heating temperature (No. 3), the level of microhardness and layer thickness grow, but even in this case, the microhardness as that on hardening of iron in LT condition is not reached, apparently, because of insufficient saturation of austenite with carbon. The complete dissolution of carbides takes place on the iron fusion (No. 4), which is accompanied by the presence of austenite stabilized too much to the martensite transformation, and the surface hardness falls. Iron in HT condition is characterized by the absence of hardness "downfall" under the hard hardened layer since the initial matrix structure (ferrite+carbides) does not undergo the transformations in the plasma heat-affected zone.

Investigation results show that the highest strengthening effect on plasma hardening of high-chromium iron is provided by the existence of the martensite+secondary carbide structure in the metallic iron matrix, and the

hardening itself does not result in the surface fusion. Therefore, plasma hardening should be integrated into the bulk surface treatment whose first stage should ensure a preset isolation of secondary carbides, which would assist the optimum austenite condition to be reached on plasma heating. The assessment of parameters of this thermal treatment and corresponding plasma hardening alternatives is of interest for further investigations.

CONCLUSIONS

1. The efficiency of plasma hardening on the surface strengthening of wear-resistant high-chromium cast irons is much dependent on their initial structure. The highest strengthening effect (matrix hardness of 1000–1080 $HV_{0.05}$) is reached for the martensite+secondary carbide microstructure, therewith plasma hardening should provide heating to 1000–1200℃ without surface fusion.

2. Plasma hardening with fusion leads to a reduction in the surface hardness of high-chromium irons irrespective of their initial microstructural condition.

3. Plasma hardening of as-cast austenite high-chromium irons is inappropriate since it does not change greatly the microstructure and hardness of the surface layer.

REFERENCES

1. A. P. Yakovlev, A. Yu. Beregovenko, V. G. Kaplun, and I. N. Pastukh, "Experimental investigation of the influence of modes of nitriding on the damping ability of 45 steel," *Strength Mater*., **29**, No. 5, 517–519 (1997).
2. A. P. Gopkalo, N. R. Muzyka, A. V. Rutkovskii, and V. P. Shvets, "Effect of PVD coatings on the strain and low-cycle fatigue resistance of stainless steel and titanium alloys," *Strength Mater.*, **43**, No. 6, 604–614 (2011).
3. S. S. Samotugin, V. I. Lavrinenko, E. V. Kudinova, and Yu. S. Samotugina, "The influence of plasma surface modification process on the structure and phase composition of cutting-tool hardmetals," *J. Superhard Mater.*, **33**, No. 3, 200–207 (2011).
4. Idris Shah Ismail Mohd and Taha Zahari, "Surface hardening of tool steel by plasma arc with multiple passes," *Int. J. Technol.*, **5**, No. 1, 79–87 (2014).
5. Y. E. Kolyada and V. I. Fedun, "Pulse electrothermal plasma accelerators and its application in scientific researches," *Probl. At. Sci. Tech.*, **98**, No. 4, 325–330 (2015).
6. V. G. Efremenko, K. Shimizu, A. P. Cheiliakh, et al., "Abrasive wear resistance of spheroidal vanadium carbide cast irons," *J. Frict. Wear*, **34**, No. 6, 466–474 (2013).
7. A. Bedolla-Jacuinde, F. V. Guerra, I. Mejia, et al., "Abrasive wear of V–Nb–Ti alloyed high-chromium white irons," *Wear*, **332–333**, 1006–1011 (2015).
8. V. Efremenko, K. Shimizu, and Yu. Chabak, "Effect of destabilizing heat treatment on solid-state phase transformation in high-chromium cast iron," *Metall. Mater. Trans. A*, **44**, No. 12, 5434–5446 (2013).
9. A. E. Karantzalis, A. Lekatou, and H. Mavros, "Microstructural modifications of as-cast high chromium white iron by heat treatment," *J. Mater. Eng. Perform*., **18**, No. 2, 174–181 (2009).
10. V. G. Efremenko, Yu. G. Chabak, and M. N. Brykov, "Kinetic parameters of secondary carbide precipitation in high-Cr white iron alloyed by Mn-Ni-Mo-V complex," *J. Mater. Eng. Perform*., **22**, No. 5, 1378–1385 (2013).
11. S. S. Samotugin, V. A. Mazur, and D. S. Litvinenko, "Simulation of thermal processes on surface plasma hardening of thin-blade cultivating tools," *Visn. SevNTU*. Ser. *Mashinopryladobud. Transport*, Issue 129, 194–198 (2012).
12. I. A. Vakulenko and V. G. Razdobreev, "Structural changes in a cold-rolled low-carbon steel during bend-tensile deformation," *Russian Metallurgy (Metally)*, No. 3, 274–279 (2004).
13. Yu. G. Chabak and V. G. Efremenko, "Change of secondary-carbides' nanostate in 14.5% Cr cast iron at high-temperature heating," *Metallofiz. Nov. Tekh.*, **34**, No. 9, 1205–1220 (2012).